High Gamma Activity in Response to Deviant Auditory Stimuli Recorded Directly From Human Cortex

Erik Edwards, Maryam Soltani, Leon Y. Deouell, Mitchel S. Berger and Robert T. Knight

JN 94:4269-4280, 2005. First published Aug 10, 2005; doi:10.1152/jn.00324.2005

J Neurophysiol 94: 4269–4280, 2005.
First published August 10, 2005; doi:10.1152/jn.00324.2005.

High Gamma Activity in Response to Deviant Auditory Stimuli Recorded Directly From Human Cortex

Erik Edwards,[1,*] Maryam Soltani,[1,*] Leon Y. Deouell,[1,2] Mitchel S. Berger,[3] and Robert T. Knight[1]

[1]*Department of Psychology and Helen Wills Neuroscience Institute, University of California, Berkeley, California;* [2]*Department of Psychology, The Hebrew University of Jerusalem, Jerusalem, Israel; and* [3]*Department of Neurological Surgery, University of California, San Francisco, California*

Submitted 29 March 2005; accepted in final form 1 August 2005

Edwards, Erik, Maryam Soltani, Leon Y. Deouell, Mitchel S. Berger, and Robert T. Knight. High gamma activity in response to deviant auditory stimuli recorded directly from human cortex. *J Neurophysiol* 94: 4269–4280, 2005. First published August 10, 2005; doi:10.1152/jn.00324.2005. We recorded electrophysiological responses from the left frontal and temporal cortex of awake neurosurgical patients to both repetitive background and rare deviant auditory stimuli. Prominent sensory event-related potentials (ERPs) were recorded from auditory association cortex of the temporal lobe and adjacent regions surrounding the posterior Sylvian fissure. Deviant stimuli generated an additional longer latency mismatch response, maximal at more anterior temporal lobe sites. We found low gamma (30–60 Hz) in auditory association cortex, and we also show the existence of high-frequency oscillations above the traditional gamma range (high gamma, 60–250 Hz). Sensory and mismatch potentials were not reliably observed at frontal recording sites. We suggest that the high gamma oscillations are sensory-induced neocortical ripples, similar in physiological origin to the well-studied ripples of the hippocampus.

INTRODUCTION

Evoked potentials provide evidence regarding the time course and neural sources of auditory processing in temporal cortices. However, limited data are available for the contribution of oscillatory activity to auditory processing. Here we examined both event-related potentials (ERPs) and oscillatory activity recorded directly from the exposed cortex of awake neurosurgical patients undergoing language mapping. We employed a mismatch paradigm in which random frequency shifts were embedded in a series of repetitive tones. The mismatch negativity (MMN) ERP, seen in response to the deviant tones, is thought to reflect automatic detection of deviance and orienting of attention (Näätänen 1992). The MMN is generated by secondary auditory cortex of the superior temporal plane (STP), somewhat anterior to the center of N1 generation (Halgren et al. 1995; Kropotov et al. 1995; Pincze et al. 2001). However, it is unknown what contribution the frontal lobe makes to the MMN.

Oscillatory neural activity in the gamma band has been a focus of interest for some time, being a putative candidate for linking disparate activity of individual neurons into both local and long-distance functional networks. Traditionally, gamma band activity was described as occurring in the range of 30–60 Hz, but newer findings suggest that oscillatory neural activity with even higher frequencies might be an important characteristic of neural activity. Grenier et al. (2001) found spontaneous "ripples" (80–200 Hz, see DISCUSSION) in the ectosylvian gyrus of cats, where feline auditory areas are located, but did not test with auditory stimulation. Induced activity ≤200 Hz has been observed after the presentation of pure tones in the auditory cortex of anesthetized monkeys (Brosch et al. 2002). In the visual system of cats, Munk and Neuenschwander (2000) have distinguished between gamma oscillations (30–60 Hz) and omega oscillations (60–120 Hz), and these are thought to arise from separate physiological mechanisms (Castelo-Branco et al. 1998; Herculano-Houzel et al. 1999; Neuenschwander and Singer 1996).

A distinction between low and high gamma in humans was originally proposed on the basis of electrocorticography (ECoG) recordings in the somatosensory and motor systems of epilepsy patients (Crone et al. 1998). Low (~35–50 Hz) and high (~70–100 Hz) gamma increases exhibited independent behavior for both cortical topography and time-course of activity. Oscillations in the high gamma band are also present in the human visual system. Early reports of visual evoked potentials to bright flashes showed fast oscillatory "wavelets" (80–170 Hz, centered at ~100 Hz) superimposed on the slower evoked potentials from ~40 to 100 ms (Allison et al. 1977; Cobb and Dawson 1960; Cracco and Cracco 1978; Vaughan and Hull 1965). A recent intracranial study employing time-frequency analyses (Lachaux et al. 2005), reported gamma power increases from 40 to 200 Hz in visual areas after the presentation of face stimuli.

A distinction between low and high gamma in the human auditory cortex was suggested by an ECoG study in epileptic patients (Crone et al. 2001). Two tones or phonemes were presented in succession in an active discrimination task. Spectral analyses at sites around the Sylvian fissure showed alpha event-related desynchronization (ERD) and low and high gamma event-related synchronization (ERS). The spatial distribution of gamma ERS was more focal than that of alpha ERD. Low gamma was less reliably obtained and did not occur at all in two patients. In contrast, high gamma ERS was reliably obtained in all patients, correlated with task specific activation, and showed distinct topographies corresponding to the two stimuli. High gamma responses to mismatch auditory stimuli have been observed up to ~90 Hz with magnetoencephalography (MEG) (Kaiser et al. 2002).

* These authors contributed equally to the work.

Address for reprint requests and other correspondence: E. Edwards, Dept. of Psychology and Helen Wills Neuroscience Inst., Univ. of California, 132 Barker Hall, Berkeley, CA 94720 (E-mail: erik@socrates.berkeley.edu).

The costs of publication of this article were defrayed in part by the payment of page charges. The article must therefore be hereby marked "*advertisement*" in accordance with 18 U.S.C. Section 1734 solely to indicate this fact.

In this study, we aimed at recording very high-frequency oscillations[1] from the exposed lateral cortex of patients undergoing awake neurosurgery, using high sampling rates and adequate filter settings. We report high gamma oscillations (60–250 Hz, centered at ~100 Hz) from left temporal areas in response to auditory tone stimuli.

METHODS

Neurosurgical patients

All patients were undergoing awake language mapping during neurosurgery for brain tumor resection (gliomas; for more details about the neurosurgical procedure, see Berger 1996 and Maciunas et al. 1996) and consented to participate in the brief auditory study after language mapping. There was no additional risk associated with this study, and it was approved by the Committee on Human Research. We recorded from 11 patients; 3 patients (data not shown) were rejected for insufficient trials completed during the procedure. Of the eight included patients (5 female and 3 male; age range, 27–56 yr), there were three frontal, three temporal, and two frontotemporal craniotomies. All craniotomies were over the left hemisphere, and all were first-time surgeries. All of the patients are anesthetized with a propofol remifentanyl combination before the language mapping. All medication was discontinued before the mapping and our study. There were no known auditory deficits in any of the patients. The right ear, facing downward, was not occluded, whereas the left ear was covered by surgical draping. The patient's hearing was not significantly compromised, allowing normal conversation with the patient during the language mapping stage of the operation.

Task and stimuli

The auditory stimuli were presented in three blocks of 500 tones, each block lasting ~3.5 min. Background noise level in the operating room was ~50–55 dB SPL; beeps of the heart rate monitor were turned off for the language mapping procedure and the experimental session. Tone stimuli were presented at ~70–75 dB SPL through speakers placed in front of and below the patient's head at ~50-cm distance. The tones were 180 ms in duration (10-ms rise-decay times; 160-ms plateau) and were presented at a rate of ~2.4 tones/s, with a pseudorandom stimulus onset asynchrony (SOA; 424 ± 29 ms). In the first and third blocks, 85% of the stimuli were standards (STAs; 500 Hz) and 15% were deviants (DEVs; 550 Hz).[2] In the second block, the standards were replaced by silences, so that deviants alone (DAs; 550 Hz) were presented (resulting in an SOA of 2,845 ± 1,128 ms, identical to the interdeviant SOA of the MMN block). The DA condition closely resembles the simple design of many early studies of the N1 (hence, we call it the "traditional" N1). Shorter SOAs, below ~1 s, are known to drastically reduce N1 amplitude and might reduce oscillatory responses as well. The purpose of the DA condition was to elicit the traditional N1 response and to serve as control to the N1 and MMN elicited by the DEV condition. The patients were instructed to ignore the sounds and look at a slide presentation of photographs.

ECoG recordings

In each of the eight patients, we recorded from five to nine epipial carbon electrodes (just under 3 mm diam), placed on the lateral surface of the temporal, frontal, and/or inferior parietal lobes. Epidural carbon electrodes placed on the margin of the craniotomy were used as the reference and ground. None of our results indicated common activity at all electrodes (which would result from activity at the reference), and all patients had at least one or two recording electrodes with no event-related activity. This indicates that the reference electrode was basically inactive with respect to this task. We preferred not to use a common-average reference (see Crone et al. 2001 for a discussion) given the small number of electrodes (5–9) used in these patients. ECoG was amplified (SA Instrumentation) with a gain of 10,000 and filter band-pass of 0.01–250 Hz (−3-dB cut-offs). Data were digitized at 2,003 Hz using Datapac 2000 software (RUN Technologies). Electrodes were already in place for the language mapping procedure, and no epileptiform activity was observed during our recordings. No electrodes placed directly over the tumor were included as confirmed by the MRI localization procedure described below.

Figure 1 shows the procedure for localizing the electrodes. Digital pictures were taken for all patients (Fig. 1, *A* and *B*), and the neurosurgeon provided gyral locations for the majority of electrodes. During surgery, the craniotomy extent was drawn on a template brain (brains in Fig. 2–4 are based directly on this template). MRI snapshots (Fig. 1*C*) were obtained for the large majority of electrodes using a frameless stereotactic device (Stealthstation, Medtronic) (Berger 1996; Maciunas et al. 1996). These MRI snapshots were subsequently aligned to the patient's MRI scan to confirm locations relative to major gyral and sulcul landmarks.

Data analysis

All data were imported into MATLAB (MathWorks) for processing. ECoG data were high-pass filtered (HPF) above 2.3 Hz with a symmetrical (phase true) finite impulse response filter (~35 dB/octave roll-off; >10 dB reduction below 2 Hz), nearly eliminating heart beat artifact. The first several tones of each block were always rejected to allow auditory responses to stabilize. Trials were rejected automatically if they exhibited amplifier saturation or excessive root-mean square voltage fluctuations. To prevent the high gamma spectral

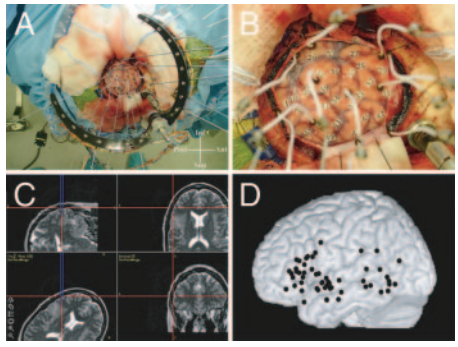

FIG. 1. ECoG methods and electrode localization. *A*: carbon electrodes are attached to a horseshoe-shaped cortical crown and placed on the pia mater. Compass in the *bottom right* indicates anatomical directions for *A* and *B*. *B*: up close image of the craniotomy depicting the electrode placements on the cortex. Electrodes on the dura mater are used as reference and ground. Numbered tags are used for language mapping purposes. *C*: MRI snapshot of each electrode position is acquired using an intraoperative localization device. Tip of an infrared probe is touched to the cortical surface and is coregistered to the patient's MRI based on geometrical triangulation with skull-affixed fiducials. *D*: electrode positions for all 8 patients. Positions were determined using the MRI snapshots and are shown on the standardized Montreal Neurological Institute (MNI) brain.

[1] It should be noted that low and high gamma activity are broadband and aperiodic, meaning that they do not appear as neatly sinusoidal oscillations. This is the case for the gamma in the present study and the other studies discussed here, and these are perhaps better described as gamma "fluctuations". This point, and its physiological significance, has been discussed previously (Engel et al. 1992), but we will continue to use the common term "oscillations".

[2] The tones were previously tested with good results in a scalp EEG study (Deouell et al. 2003). Note that the relatively low frequencies of the tones used here are likely to activate more lateral portions of auditory cortex within the STP, given what is known about tonotopic organization in humans.

results from being influenced by outlier activity, trials were also automatically rejected if they contained outlier (3 SD) high gamma power or high gamma power changes. This conservative approach seems appropriate considering the exploratory nature of this study and the novelty of the findings. It ensures that what we report is a typical physiological response rather than a result caused by a few highly abnormal physiological or nonphysiological events. Only a handful of trials were rejected by this criterion, and it made no material difference for any of the results shown. Finally, noisy channels and data segments were rejected manually using EEGLAB (Delorme and Makeig 2004).

ERPs, taken as the averages relative to tone onset, were made for each channel and tone type separately. To assess whether an ERP differed significantly from the baseline, we used the same resampling analysis described below for the time-frequency data. This resulted in a time series of raw P values indicating the percentile position within the surrogate distribution drawn from the single trial baseline data. As with all P values reported here, we corrected for multiple comparisons using the false discovery rate (FDR) approach (Benjamini and Hochberg 1995). This approach has a number of advantages for exploratory data analysis (for discussion, see Nichols and Hayasaka 2003).

Individual temporal and posterior Sylvian electrodes with significant N1 potentials (i.e., a significant peak in the latency range of the N1) in both the DEV and DA responses were tested further for significant amplitude and latency differences between these two conditions (Fig. 2, *E* and *F*). This was done using a permutation test as follows. Individual trials from the two conditions (DEVs and DAs) were pooled together. For each of 5,000 iterations, two groups of trials were drawn at random without replacement from this pool to represent the DEV and DA conditions, with the appropriate number of trials in each group as in the original samples. Distributions were created from the peak amplitude and latency differences between these surrogate ERPs, calculated at each iteration. The actual peak amplitude and latency differences were tested against these distributions to see if they were likely to have arisen by chance ($P < 0.05$, 2-sided, FDR corrected for multiple comparisons because 13 electrodes with prominent N1s were tested).

Time-frequency analyses used a 256-point, Hanning-tapered, moving-window fast Fourier transform (FFT) on the single-trial data, followed by averaging across trials. The window was advanced in four sample point steps to give 274 output times per trial, and the frequency bin width (Δf) was 3.91 Hz. Outputs at each time-frequency point are shown in units of decibels ($\mathrm{dB} = 10 \log_{10}$) relative to the mean power spectrum in the baseline period. These event-related spectral perturbations (ERSPs) emphasize proportionate poststimulus amplitude changes without obscuring by noisy epochs of overall power elevation (Makeig 1993). The complex FFT output was also used to calculate intertrial coherence (ITC). For each latency and frequency bin, the normalized vectors (unit length) in the complex plane were averaged across trials. The length of the resulting vector is the ITC and ranges from 0 to 1. If there is a high degree of phase consistency across trials, the unit vectors will align and average to a larger vector than if they are scattered around the phase circle. High versus low ITC corresponds to evoked versus induced activity.

Significance of poststimulus increases and decreases in spectral power were tested at each frequency using the resampling method of Makeig and colleagues (Delorme and Makeig 2004; Makeig et al. 2002). Data points were drawn at random from the prestimulus baseline periods of the single-trial data to create the reference distribution. Raw P values were obtained as percentiles within this baseline distribution. P values still significant after FDR correction for multiple comparisons ($P < 0.02$, 2-sided) are indicated directly on the ERSP plots by the outermost contour lines. To assess amplitude and latency differences between conditions in the ERSPs, a similar permutation test as described above for the ERPs were used except using the dB time series of a chosen frequency band rather than the voltage time series (ERP).

RESULTS

The most prominent tone-locked ERP responses were obtained at sites surrounding the posterior extent of the Sylvian fissure. All posterior Sylvian electrodes showed an ERP referred to as the N1 because its latency (~100 ms) and polarity reversal across the Sylvian fissure (Fig. 2*A*) strongly suggest that it corresponds to the well-known vertex maximal scalp N1 response. The major generators of the N1 are located in the auditory cortices of the STP within the Sylvian fissure (Näätänen and Picton 1987; Jääskeläinen et al. 2004). In addition to these far-field voltages, however, local generators beneath the electrodes probably made contributions to the ERP responses seen. The N1 response was often preceded by a smaller potential of opposite polarity corresponding in latency to the P1 (latency of ~70 ms) and was often followed by slower potentials possibly corresponding to the auditory P2 or N2 responses. All of these potentials were generally found to be larger at sites inferior to the Sylvian fissure. This may be because of the presence of local generators within the lateral temporal cortex. In several electrodes, we saw evidence for components previously suggested to be generated in the lateral temporal cortex (i.e., the T-complex or the N1a and N1c; Knight et al. 1988; Wolpaw and Penry 1975). The N1 was the most reliable ERP, and only this potential will be discussed further.

In most posterior Sylvian electrodes, the N1 amplitude was significantly larger for DEV tones compared with STAs and was significantly larger for DA tones than for DEVs (Fig. 2*E*). This trend was evident in all posterior Sylvian electrodes (9 electrodes in 3 patients) showing a significant N1, but was significant ($P < 0.05$) in only six electrodes in two patients. There was also a significant ($P < 0.05$) latency shift between the N1 peak for DAs (~95 ms) compared with DEVs (~115 ms) in 10/13 electrodes (Fig. 2*F*). In Fig. 2*E*, the N1 peak amplitude is sorted as a function of anterior-posterior electrode position. In the posterior half of electrodes, DA responses dominate and some STA responses are seen. In the anterior half of electrodes, DEV and DA responses are similar in amplitude, and little or no STA responses are seen. We calculated a center-of-mass (COM; Fig. 4, *1st row*), and the DEV COM was significantly anterior to the DA COM. However, this anterior-posterior distinction is only presented as a trend because these analyses are done across subjects (5 subjects with different exposures and different numbers of electrodes). A stronger confirmation is provided by an individual patient with extensive exposure of the STG including both anterior and posterior STG electrodes (Fig. 2*B*; patient 9). In this patient, the response to the DA is strongest at the most posterior electrode and is absent in the two most anterior electrodes, whereas the response to the DEV becomes stronger than the response to the DA at the more anterior electrodes. In fact, in the two most anterior sites, only the DEV response can be seen.

Despite recording from 23 frontal electrodes in 5 patients, ERP responses significantly different from baseline were rarely obtained (Fig. 2*C*). The five most likely examples of positive results obtained in the frontal lobe are shown in Fig. 2*D*. These were small in amplitude, and at least one was likely a far-field

potential of reversed polarity of a temporal electrode. Thus no conclusive ERP result was obtained in any of our frontal recordings.

The time-frequency results, obtained with a moving-window FFT (see METHODS), are shown in Fig. 3 for several temporal electrodes. There are three major aspects of the ERSP obtained for DEVs and DAs. First, there was an increase in the power of frequencies <40 Hz that was coherent across trials (Fig. 3, ITC plots). This response began earliest (~30- to 55-ms peak) in the 20- to 40-Hz band and spread into the frequencies <20 Hz over the next ~40 ms. This likely corresponds to the middle-latency auditory evoked potentials (MAEPs) and P1, which have frequency content between 20 and 40 Hz, followed by the N1 response as seen in the spectral domain. In several electrodes (e.g., Fig. 3, patient 8), there is a second power increase in the frequencies <20 Hz that follows this first increase by ~180 ms. This is the duration of the tone stimulus, so it is probably a tone offset response.

Second, there was a decrease in power (i.e., ERD) in the frequencies <30 Hz beginning at ~140 ms after the tone. This usually appeared somewhat earlier in the beta band. Alpha

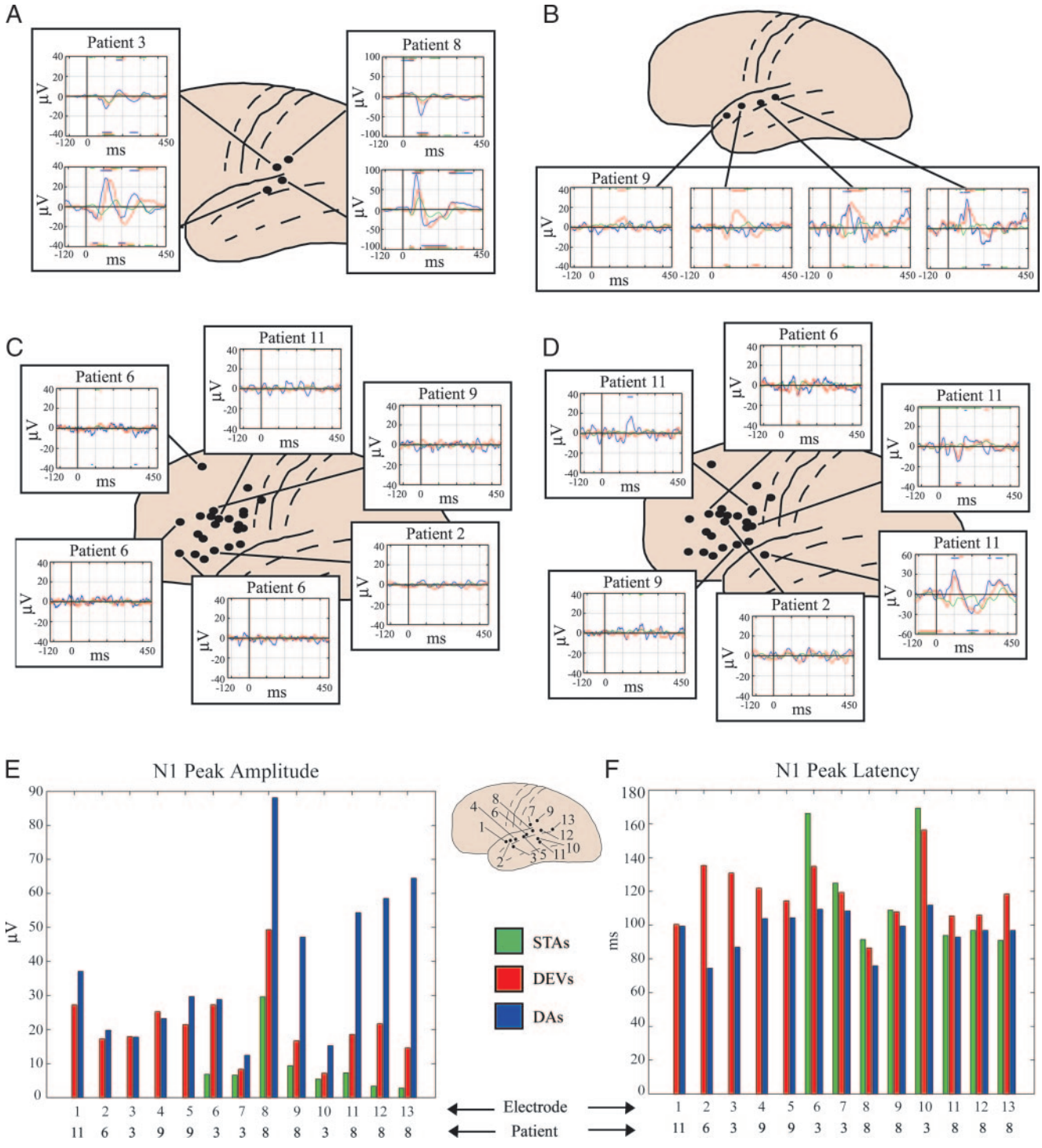

ERD in particular was seen at widespread electrodes ranging from temporal-occipital to prefrontal cortices (Fig. 4). Alpha ERD was occasionally obscured by the above-mentioned offset response.

The third and most striking time-frequency result was a large "island" of induced activity in the low gamma (30–60 Hz) and high gamma (60–250 Hz) bands[3] from ~35 to 350 ms. There are two reasons to consider the low and high gamma bands as distinct. The high gamma activity generally had an earlier onset than the low gamma activity, and the activity in the high gamma band appeared in the absence of low gamma activity at some electrodes (Fig. 3, patients 3 and 11). Significant high gamma activity was seen as high as 250 Hz (Fig. 3, patient 8) but was always strongest below ~160 Hz. The frequency band of maximum response could appear anywhere from 70 to 160 Hz but was usually around 100 Hz (100 ± 20 Hz across 17 temporal and posterior Sylvian electrodes). The power augmentation (i.e., ERS) in the high gamma band reached levels as high as 11.6 dB relative to baseline, corresponding to a 280% increase in signal amplitude (or a 1,350% increase in power).

It might be argued that the high gamma increase merely represents the high-frequency components of the ERPs, namely steep slopes or sharp peaks within the single-trial waveforms that are not present in the final ERPs because of latency jitter. However, the rising slope of the N1 is steeper than the falling slope, and the fastest ERPs occur in the interval before the N1. In contrast, the high gamma increase is maximal during the falling slope of the N1 and in the ensuing ~100 ms. This is true not only in the averages but also in the single-trials. The duration of the high gamma increase and examination of some single-trial data (Fig. 3, patient 8) also strongly suggest that this increase is caused by multi-cycle fluctuations and not by sharp features of the ERPs.

The spectral changes share several common features with the ERP findings. First, at more posterior electrodes, the spectral changes were strongest for DA tones and weakest for STA tones, with DEV tones giving intermediate levels of spectral activity (as exemplified by Fig. 3, patient 8). This pattern (STA < DEV < DA) was generally found for the high gamma and alpha ERD, but it did not hold at all posterior electrodes. For example, Fig. 3, patient 3, showed the pattern STA < DEV = DA for high gamma, and the alpha ERD results from patient 8 were often confounded by a strong offset response. DEVs showed stronger activity than DAs at some more anterior temporal electrodes (Fig. 3, patient 11). Consequently, these spectral changes were more anteriorly distributed along the extent of the Sylvian fissure for the DEVs than for the DAs. This was assessed with a simple COM (i.e., center-of-activity) calculation and is shown in Fig. 4, *right column*. Both the ERPs and the high gamma had more anterior DEV COMs compared with the DA condition ($P < 0.01$). Second, the latencies of spectral power changes tended to be earlier for DA tones than for DEVs, although no differences reached significance after correction for multiple comparisons. The lack of statistical significance of this trend could be the result of the difficulty to precisely determine the latency within an island of spectral power change. Third, much weaker responses were obtained at frontal electrodes compared with temporal electrodes. As seen in Fig. 4, only alpha ERD extended with any significant amplitude into frontal electrodes. These were concentrated in the posterior half of the inferior frontal gyrus. Weak (<1 dB) but significant gamma activity was obtained at a few frontal recording sites. Overall, we were unable to observe robust high gamma activity at frontal sites.

[3] There is often a trough of activity at ~60 Hz in the time-frequency plots such that there appears to be separate islands of activity above and below 60 Hz. This is almost certainly due to line noise artifact. The boundary between low and high gamma at ~60 Hz was based on previous findings (Discussion). The frequency bin including 60 Hz was not used in any of our subsequent analyses.

DISCUSSION

ERP findings

The major generator of the scalp-recorded auditory N1 potential is located within the STP (Godey et al. 2001; Knight et al. 1980; Näätänen and Picton 1987). Consistent with these results, we observed a polarity inversion of the N1 across the Sylvian fissure. Source analyses of the scalp-recorded EEG have shown that the MMN is generated by secondary auditory cortex of the STP (Giard et al. 1990; Scherg et al. 1989). MEG recordings in humans (Hari et al. 1984), and intracranial recordings in animals (Csépe et al. 1987; Javitt et al. 1994; Kraus et al. 1994) and humans (Kropotov et al. 1995; Liasis et al. 2000) have supported these results. Our results support the origin of a response to rare or deviant stimuli from the more anterior auditory cortices within the STP and/or along the STG.

It is unknown what the frontal lobe contributions are to the MMN. Scalp current-source density (CSD) analyses suggest

FIG. 2. Event-related potentials (ERPs). Green traces, standard tones (STAs; 500 Hz); red traces, deviant tones (DEVs; 550 Hz); blue traces, 550-Hz tones (DAs) presented alone in a separate block. Lines above and below the traces indicate that the ERP is significantly different from baseline ($P < 0.02$). *A*: ERPs from 2 patients that had electrodes above and below the posterior Sylvian fissure. The main ERP seen at ~100-ms latency reverses polarity across the posterior Sylvian fissure, indicating that the major source is within the superior temporal plane. We refer to this potential as the N1. *B*: ERPs from a single patient that had electrodes arrayed along the anterior-posterior extent of the STG. Response to DEVs extends further anteriorly than the response to DAs. Note that these are among the noisiest temporal ERPs obtained. *C*: 6 examples of negative results in frontal regions. These are typical of the majority of electrodes recorded from frontal sites. *D*: 5 frontal electrodes with the most prominent responses are shown. Positive deflection at ~170 ms in patient 11 (electrode in *top left*) is the largest response we observed of all frontal recordings (23 electrodes total across 5 patients with frontal exposure). However, this is not the appropriate latency or polarity to contribute to the N1 or MMN. Electrode from patient 11 in the *top right* shows a negative deflection that at 1st seems compatible with N1 or MMN generation. However, comparison with a temporal electrode from the same patient (*bottom right*) indicates that this is a far-field effect exhibiting polarity reversal accross the Sylvian fissure. Electrodes from patients 6 and 9 show a slight (<10 μV) negative deflection at a latency appropriate for the N1 or MMN (~95–125 ms). However, this only attains significance in the DEV response for patient 6, and a far-field origin similar to that shown for patient 11 cannot be ruled out. Electrode from patient 2 shows a small positive deflection at ~90 ms that does not attain significance. *E*: N1 peak amplitudes from the 13 temporal and peri-Sylvian electrodes that showed significant N1 responses. Electrode locations are shown on the inset brain, and numbering is in order of most anterior to most posterior. It can be seen that the DA responses are much stronger in the more posterior electrodes (significantly greater than DEV responses in 5 of the posterior 6 electrodes; $P < 0.05$), whereas the DA and DEV responses are similar in the more anterior electrodes (no significant differences in the anterior 7 electrodes). *F*: N1 peak latencies, showing that the DEV response is longer in latency in all 13 electrodes (significant in 10/13; $P < 0.05$).

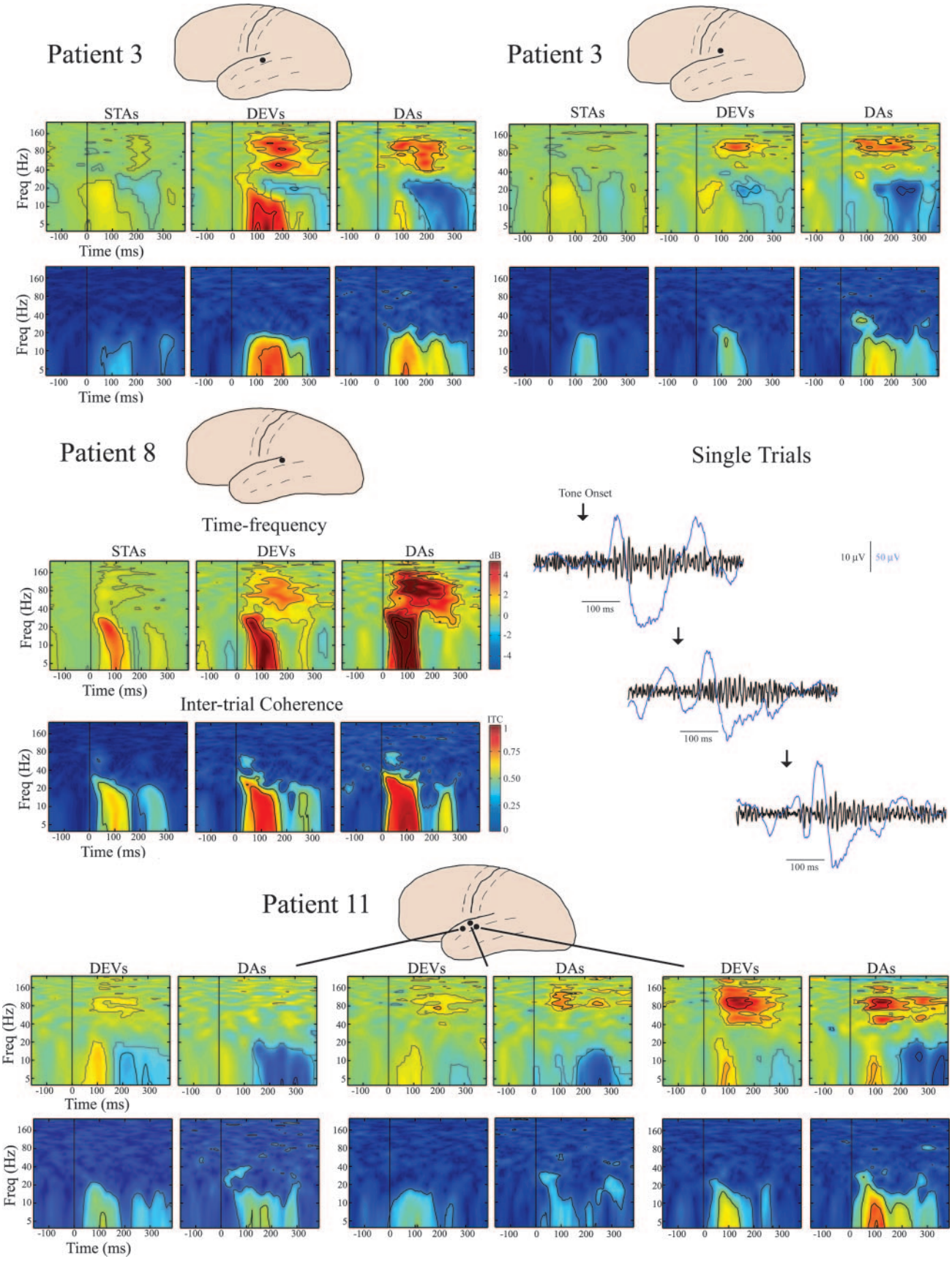

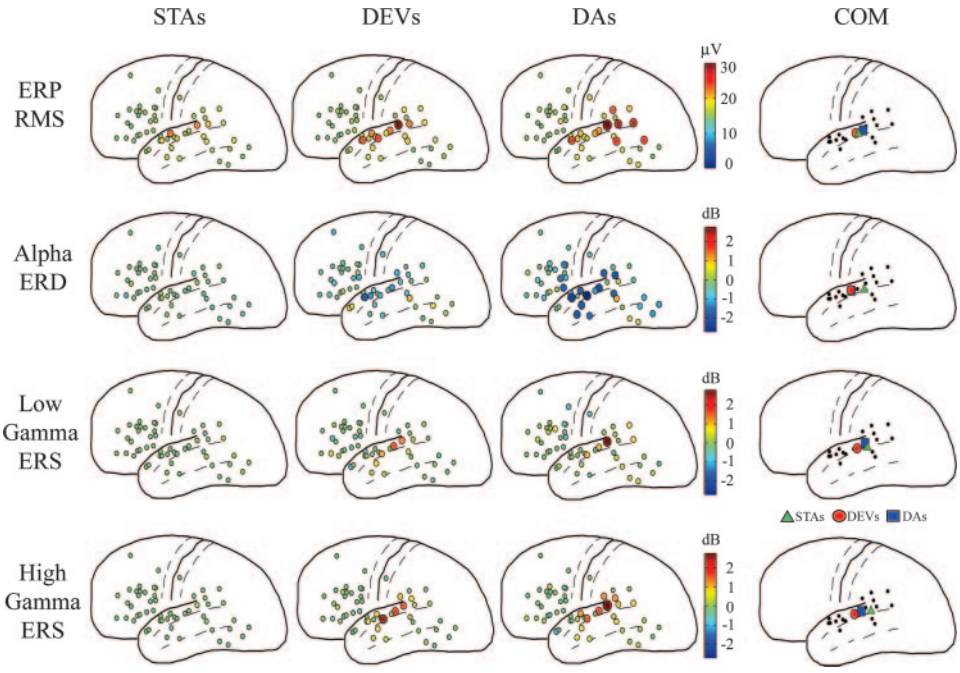

FIG. 4. Summary of the anatomical distribution of ERP and time-frequency activity. On each brain template, circles indicate the nonrejected electrodes from all 8 patients. Size and color of each circle is proportional to the level of activity seen at that site (scale shown in color bars to the *right*). The 1st row of brain templates characterizes overall ERP activity with the root-mean-square (RMS) of significant ERP time-points over the interval 25–200 ms. The 2nd row shows level of poststimulus power suppression (ERD) in the alpha (7–12 Hz) band. The 3rd and 4th rows show levels of low (35–55 Hz) and high gamma (70–160 Hz) power augmentation (ERS). For the gamma bands, these were calculated as the mean dB level from 25 to 300 ms after stimulus onset. For the alpha band, the time interval extended from the 1st nonpositive time-point (156 ± 105 ms) to 385 ms. Activity for each tone type (STAs, DEVs, DAs) are shown in separate columns. The more anterior distribution of activity for the DEV condition is clearly seen in these summary templates. To better quantify this, a "center-of-mass" (COM) was calculated for each tone type, and these are shown in the 4th column. This calculation was restricted to auditory-responsive areas around the STS and posterior Sylvian fissure (electrodes indicated by black dots). The most anterior COM is always from the DEV condition. This was tested for significance by computing the anterior-posterior COM difference for each of 5,000 bootstrap iterations. For the high gamma, the DEV COM was significantly anterior to both the DA and the STA COMs ($P < 0.01$, 2-tailed, FDR-corrected). For the ERPs, the DEV vs. DA difference was significant, and for low gamma, this difference approached significance ($P = 0.056$).

that, in addition to contributions from the left and right STP, the frontal cortex also contributes to the scalp-recorded MMN (Deouell et al. 1998; Giard et al. 1990; Rinne et al. 2000; Serra et al. 1998). However, although CSD derivations are more sensitive to cortical sources than to deep sources, they do not provide fine grained estimates of the exact origin of activity. Several fMRI studies employing a passive oddball paradigm have also found frontal activity related to the occurrence of a deviant, especially in the inferior frontal gyrus (Doeller et al. 2003; Opitz et al. 1999, 2002). However, because of the poor temporal resolution of the method, it is difficult to ascertain whether this activity was elicited at the latency window of the MMN or at a later time. Finally, two human lesion papers provided evidence that prefrontal cortex modulates MMN generation by showing that patients with discrete lesions in dorsolateral prefrontal cortex have diminished MMN responses (Alain et al. 1998; Alho et al. 1994). These results could be explained by a top-down effect on the STP activity rather than a frontal generator of the MMN.

Intracranial evidence for a frontal generator of the MMN is scarce and inconsistent. In the extensive depth recordings of Halgren and colleagues (Baudena et al. 1995; Halgren et al. 1995), no frontal MMN was reported. Their studies, however, were not intended or designed specifically to look for the MMN. In a case study of a 6-yr-old child (Liasis et al. 2001), ECoG was recorded over the left and right prefrontal cortex, and an ERP corresponding to the MMN was observed at contacts over the right hemisphere. A recent study of 29 adult patients found 2 patients with a weak mismatch response over left inferior frontal cortex (Rosburg et al. 2005), but the possibility of volume conduction from anterior temporal areas was not considered (as in our patient 11, Fig. 2*D*).

Our study uses a task specifically designed to elicit the MMN, and our recording electrodes were placed over both

FIG. 3. Time-frequency results from 3 patients. Electrode positions for each patient are indicated on the brains above the graphs. In each group, the *top row* shows the event-related spectral perturbations (ERSPs) and the *bottom row* shows the intertrial coherences (ITCs). In all plots, absicca gives time relative to tone onset and ordinate gives frequency of the ECoG. ERSPs show the power in each frequency band in units of dB relative to prestimulus baseline. Color scale, which is the same for all ERSPs, is given in the color bar next to the ERSPs for patient 8. Outer contour lines in each ERSP enclose time-frequency pixels that are significant relative to baseline ($P < 0.02$). Additional contour lines are drawn at 2-dB increments (≤10 dB in patient 8). In the ITC plots, contour lines are drawn at the levels specified by tick marks in the color bar, but do not indicate statistical significance. These show the much stronger intertrial phase consistency for lower frequency bands (< ~30 Hz) compared with the higher frequency bands (i.e., the gamma activity is "induced"). Some examples of single-trial waveforms are shown for the electrode from patient 8, all from the DA condition. Blue trace shows broadband data (HPF at 2.3 Hz) as used for all analyses. These show the large trial-to-trial variability of the evoked response (Zerlin and Davis 1967). Black trace shows data filtered to isolate fluctuations in the high gamma range (HPF at 75 Hz). High gamma fluctuations occur mainly during the falling phase of the N1 and after. These can also be seen in the broadband waveforms (blue traces) on close examination (note the different voltage scales for blue and black traces).

frontal and temporal areas in several adult patients. Although we did not observe a frontal MMN, our electrodes were placed only over the left hemisphere. Because of the nonuniform (predominantly ventro-latreral frontal) distribution of electrodes in our recordings, it cannot be excluded that a left frontal generator exists but was missed. Thus the question of a frontal MMN generator remains unresolved.

Time-frequency findings

Spectral analysis is nearly absent in intracranial auditory studies to date. Crone et al. (2001) have shown the responses of select frequency bands in ERP-style traces. The full time-frequency plane, as presented here, better delineates the temporal evolution of activity in all frequency bands in response to auditory stimuli. We identified five aspects of the time-frequency responses to DEV and DA tones at sites surrounding the posterior Sylvian fissure (Fig. 3).

There is a significant increase in the power between ~20 and 40 Hz from ~15 to 100 ms that is coherent (phase-locked) across trials. The MAEPs and the P1 occur during this latency range. The temporal structure of the MAEPs is such that they exhibit spectral energy in the range of ~30–50 Hz (Galambos et al. 1981; Suzuki et al. 1983), and they appear as auditory "evoked gamma" in time-frequency analyses. With tones of moderate rise-time instead of clicks, the latencies of MAEPs are somewhat prolonged and the frequency composition would be somewhat lower. MAEPs from monkey auditory cortex in response to tones showed a spectral content between ~20 and 40 Hz (Brosch et al. 2002). Thus we conclude that the observed activity is the correlate of the scalp recorded MAEPs.

The lower frequencies (<20 Hz) subsequently (~50–150 ms) show a strong power increase, which is also coherent across trials. The major portion of this power increase is likely caused by potential changes associated with the N1 and the neighboring long-latency AEPs P1 and P2. In any case, the ERPs obtained must have resulted from activity in these lower frequency bands because a high ITC is a prerequisite for the appearance of an ERP. In contrast, the high gamma and low gamma after the early MAEP/P1 interval showed very low ITC (i.e., they were "induced") and therefore could not have contributed significantly to the ERPs.

Beginning at ~160 ms and continuing up to >400 ms poststimulus, there is a decrease in low-frequency power (<30 Hz). Alpha and beta ERDs have been described many times in visual and sensorimotor studies (Pfurtscheller and Lopes da Silva 1999) and occasionally in auditory studies using scalp EEG (Krause et al. 1994; Pfurtscheller and Aranibar 1977) and MEG (Lehtela et al. 1997; Tiihonen et al. 1991). Indeed, the earliest studies of the human auditory EEG reported blocking of the alpha rhythm to auditory stimuli (Berger 1930; Davis 1939; Durup and Fessard 1935). Our observation of widespread alpha ERD, ranging from prefrontal to temporal-occipital cortices, is in accord with these early observations. To our knowledge, only one intracranial study has reported ERD after auditory stimulation (Crone et al. 2001). As in their prior somatomotor study (Crone et al. 1998), the alpha ERD was widespread compared with gamma ERS. Alpha ERD is considered a general indication of cortical activation, along with more specific gamma increases. The term "desynchronization" implies that the decrease in power is caused by a decrease in coherence across space rather than a genuine suppression of power at the level of elementary generators. ECoG sums over an order of magnitude fewer cortical columns than scalp EEG, so it is possible that the alpha ERD of this study involves more than just a decrease in coherence across space.

Induced low gamma (30–60 Hz) activity appears between ~90 and 290 ms. In Fig. 3, we show three examples of prominent high gamma without corresponding low gamma activity, but we do not find in our data set an example of low gamma in the absence of high gamma. Crone et al. (2001) have also noted that low gamma is less reliably obtained than high gamma.

Preceding the low gamma in latency (onset of significant activity at ~35–95 ms) is a broadband burst of activity in the high gamma range, here taken as 70–160 Hz.[4] The frequency with the strongest response is ~100 Hz for both DEVs and DAs. This high gamma is strongest at the temporal sites and weak and inconsistent at the frontal sites. The possible origin and significance of high gamma activity is discussed below.

Low gamma versus high gamma

The high gamma activity often begins earlier and peaks earlier than the low gamma activity, indicating that the high gamma is not just "spectral splatter" of the low gamma activity. Nor does the peak frequency of the high gamma appear as a simple resonant frequency of the low gamma peak. In some individual electrodes (Fig. 3), high gamma activity can appear in the near absence of low gamma activity or the latencies can be quite different. These considerations indicate that distinct mechanisms underlie high and low gamma activity. Crone et al. (2001) also reached the conclusion that high and low gamma represent independent physiological mechanisms. Overall, these results agree with the auditory results of Crone et al. (2001) in almost every respect, despite task differences (passive listening vs. active discrimination), patient differences (tumor patients vs. epilepsy patients), and recording and analysis differences. These findings extend previous ones in showing that the high gamma activity can be generated without voluntary attention and active discrimination of the auditory stimuli.

The physiological origins of auditory gamma have been studied in most detail in the rat by Barth and colleagues (Barth and Macdonald 1996; Sukov and Barth 1998). Their studies indicate that spontaneous and auditory-induced low gamma oscillations reflect the same sequence of interlaminar activations as the rat MAEPs (P1-N1) (Sukov and Barth 1998). Excitatory input to supragranular pyramidal cells yields the P1 or the gamma positive phase, followed by input to apical dendrites of infragranular cells yielding the N1 or the gamma negative phase (positive/negative potential at the cortical surface). Multiple cycles of these type A and type C activations (Mitzdorf 1985) appear as low gamma frequency oscillations. Thus low gamma directly reflects postsynaptic potentials (PSPs) in cortical pyramidal cells. By analogy to what is known

[4] The full high gamma range where power increases were observed is 60-250 Hz. The range wherein the strongest activity was contained, as well as the range of peak frequencies, was 70-160 Hz. This also corresponds approximately to the range of inter-peak intervals in the single-trial oscillations, which is a common method of identifying frequency range in the animal studies cited here. Thus, we will use the range 70-160 Hz for this discussion.

known about hippocampal and neocortical ripples, high gamma may reflect inhibitory PSPs (IPSPs) and/or summated action potential (AP) currents.[5]

Ripples in hippocampus and neocortex

Fast field potential oscillations in the hippocampus termed "ripples" (125–250 Hz) were first observed in wideband microelectrode recordings from unanesthetized rats (O'Keefe 1976; O'Keefe and Nadel 1978; Suzuki and Smith 1988). Intracranial recordings from unanesthetized humans have shown hippocampal ripples with a lower frequency of ~80–160 Hz (Bragin et al. 1999a; Staba et al. 2002), which is similar to the high gamma range reported here (70–160 Hz).

The physiological correlates of hippocampal ripples have been studied extensively in rats. Ripples are most often superimposed on slower "sharp waves" (SPWs) and hence are associated with a period of excitation, neuronal depolarization, and population bursts of pyramidal cells (Buzsáki 1986; Suzuki and Smith 1988; Ylinen et al. 1995). Although individual pyramidal cells do not always fire at each peak of the ~200-Hz ripple, the time-course of the population firing rate exhibits ~200 Hz rhythmicity (in rats, Buzsáki et al. 1992). The synchronous AP currents associated with these population discharges may summate to produce the oscillations in the field potentials. Interneurons show an even stronger coupling with the field ripples, often discharging with each oscillatory cycle. Based on this fact, as well as current-source density analyses and intracellular results, synchronous $GABA_A$-mediated IPSPs on the perisomatic regions of pyramidal cells have also been proposed as the immediate source of ripples (Ylinen et al. 1995). Thus ripples are a direct reflection of synchronous AP- and/or IPSP-associated currents.

The mechanism by which the hippocampal network gives rise to ripple oscillations probably involves electrical coupling through axo-axonal gap junctions (Draguhn et al. 1998; Traub et al. 1999, 2003), as evidenced, for example, by the disappearance of ripples with gap junction blockers like halothane. An additional role is played by network interactions mediated by fast (AMPA, $GABA_A$) chemical synaptic transmission (Brunel and Wang 2003; Maier et al. 2003; Traub and Bibbig 2000), whereas slower receptor types [*N*-methyl-D-aspartate (NMDA), $GABA_B$] and intrinsic membrane oscillations (Ylinen et al. 1995) do not contribute to ripple frequency oscillations. Hippocampal ripples and low gamma (30–60 Hz) are considered distinct phenomena (Chrobak et al. 2000; LeBeau et al. 2003).

Neocortical ripples (80–200 Hz) have been observed in multiple sensory and association cortices of the cat with and without anesthesia and during both sleep and waking (Grenier et al. 2001). Without anesthesia, these neocortical ripples occurred most often during the depth-negative phase of the slow oscillations of slow-wave sleep. This is a period of excitation and neuronal depolarization, similar to the association of hippocampal ripples with excitatory SPWs. Other observations support a close relation to hippocampal ripples. For example, ripples were reversibly blocked by the gap junction blocker halothane, and intracellular recordings with KCl filled pipettes indicated involvement of $GABA_A$-mediated IPSPs. It was proposed that a combination of inhibitory synaptic currents and synchronous AP currents contributed directly to the neocortical field ripples.

Cat neocortical ripples were reported at a somewhat lower frequency (80–200 Hz) than the rat hippocampal ripples described above, possibly representing a species difference. Ripples, originally termed "minispindles," are observed in the cat hippocampal system at a lower frequency (85–155 Hz) than in rats (Collins et al. 1999; Eguchi and Satoh 1987; Kanamori 1985, 1986). Cat and human hippocampal ripples occur in the same frequency range, suggesting that human neocortical ripples may appear in the range seen for cats. In support of this, neocortical ripples preceding epileptic seizures in cats (Grenier et al. 2003) and humans (Fisher et al. 1992; Traub et al. 2001) are found with a similar frequency range. Thus the high gamma reported here (60–170 Hz, centered at 100 Hz) is in the predicted range for human neocortical ripples. This link is tentative because the cat studies of neocortical ripples did not use sensory stimulation.

Although the various field potential oscillations in the high gamma range discussed above are of uncertain relationship to each other, they provide ample precedent for the existence of cortical oscillations above the traditional low gamma range, which arise from separate physiological mechanisms as low gamma.

Origins and significance of high gamma

High gamma and ripples are not the highest oscillatory phenomena known. Another set of field potential oscillatory phenomena that are caused by synchronous AP currents is found above the range of ripples and high gamma (i.e., above ~200–250 Hz). These include the pathological fast ripples (250–600 Hz) of human and rat epileptic hippocampus (Bragin et al. 1999b), the σ-bursts (~600 Hz) of somatosensory cortex evoked by electrical stimulation of peripheral nerves (Baker et al. 2003; Cracco and Cracco 1976; Curio et al. 1994), the I-waves (~600 Hz) of the motor cortex evoked by direct electrical or magnetic stimulation (Amassian and Stewart 2003; Mingrino et al. 1963; Patton and Amassian 1954), and fast oscillations (~300 Hz) in rat auditory and somatosensory cortices (Jones and Barth 1999, 2002; Staba et al. 2003). In each of these cases, the direct generating mechanism is currently thought to be population spiking of pyramidal cells and the consequent summation of AP currents (including terminal fields of APs in thalamocortical fibers). Below the range of high gamma and ripples lies the traditional gamma range, here termed low gamma. Low gamma field oscillations in the hippocampus (Buzsáki et al. 1983; Csicsvari et al. 2003) and neocortex (Sukov and Barth 2001) are the direct reflection of summated excitatory PSPs (EPSPs) and IPSPs. Indeed, the majority of EEG phenomena in the range of ~2–60 Hz are thought to be caused (directly) by summated PSPs on pyramidal cells (Creutzfeldt and Houchin 1974; Elul 1971; Mitzdorf 1985). Thus high gamma is bounded above by a set of phenomena directly caused by AP currents and bounded below by a set of phenomena directly caused by PSP currents. Deter-

[5] To clarify, most studies of ripples emphasize the role IPSPs in their generation, whereas Barth's studies of low gamma emphasize the role of EPSPs. But IPSPs have also been proposed to contribute to low gamma, and it cannot yet be excluded that EPSPs contribute partly to ripples. The difference may be in the relative contributions of these two and in the role of AP currents, see Discussion.

mining the relative contributions of these two sources to high gamma will be critical to elucidating its mechanism of generation.

Each of the high-frequency oscillations discussed thus far have been ascribed a similar overall functional significance. They are all thought to reflect an underlying temporal structure and coordination of population activity (Barth 2003; Chrobak and Buzsáki 1998; Neuenschwander et al. 2002; Sannita 2000), playing an important role in neural coding by assembly formation and neural communication by collective signaling, as also discussed previously for low gamma oscillations (Buzsáki et al. 1994; Singer 1993). We suggest that the high gamma activity reported here plays a similar functional role in the auditory system of humans.

In conclusion, salient auditory stimuli elicit distinct ERPs on the superior temporal plane, with deviancy ERPs located in more anterior regions of the STP. Salient and deviant events also elicit oscillatory activity in several frequency bands. These activities extend to the high gamma range in latencies starting around the time that information arrives at the auditory cortex. Given the passive nature of this experiment, it appears that goal-directed processing of stimuli is not necessary for eliciting high gamma activity. Rather, it can be elicited automatically by salient stimuli. Further studies in humans and in animal models are needed to understand the generating mechanisms of high gamma and its relation to other high-frequency field potential phenomena in the cortex.

ACKNOWLEDGMENTS

The authors thank S. Makeig, R. Fechter, C. Clayworth, A. Leong, and H. Clay for their assistance.

GRANTS

This study was supported by National Institute of Neurological Disorders and Stroke Grant NS-231135 and the Rauch family.

REFERENCES

Alain C, Woods DL, and Knight RT. A distributed network for auditory sensory memory in humans. *Brain Res* 812: 23–37, 1998.

Alho K, Woods DL, Algazi A, Knight RT, and Näätänen R. Lesions of the frontal cortex diminish the auditory mismatch negativity. *Electroencephalogr Clin Neurophysiol* 91: 353–362, 1994.

Allison T, Matsumiya Y, Goff GD, and Goff WR. The scalp topogrphy of human visual evoked potentials. *Electroencephalogr Clin Neurophysiol* 42: 185–197, 1977.

Amassian VE and M. Stewart. Motor cortical and other cortical interneuronal networks that generate very high frequency waves. *Suppl Clin Neurophysiol* 56: 119–142, 2003.

Baker SN, Curio G, and Lemon RN. EEG oscillations at 600 Hz are macroscopic markers for cortical spike bursts. *J Physiol* 550: 529–534, 2003.

Barth DS. Submillisecond synchronization of fast electrical oscillations in neocortex. *J Neurosci* 23: 2502–2510, 2003.

Barth DS and Macdonald KD. Thalamic modulation of high-frequency oscillating potentials in auditory cortex. *Nature* 383: 78–81, 1996.

Baudena P, Halgren E, Heit G, and Clarke JM. Intracerebral potentials to rare target and distractor auditory and visual stimuli. III. Frontal cortex. *Electroencephalogr Clin Neurophysiol* 94: 251–264, 1995.

Benjamini Y and Hochberg Y. Controlling the false discovery rate - a practical and powerful approach to multiple testing. *J Roy Stat Soc Ser B* 57: 289–300, 1995.

Berger H. Über das elektrenkephalogramm des menschen. *J Psychol Neurol* 40: 160–179, 1930.

Berger MS. Minimalism through intraoperative functional mapping. *Clin Neurosurg* 43: 324–337, 1996.

Bragin A, Engel J Jr, Wilson CL, Fried I, and Buzsáki G. High-frequency oscillations in human brain. *Hippocampus* 9: 137–142, 1999a.

Bragin A, Engel J Jr, Wilson CL, Fried I, and Matern GW. Hippocampal and entorhinal cortex high-frequency oscillations (100–500 Hz) in human epileptic brain and in kainic acid–treated rats with chronic seizures. *Epilepsia* 40: 127–137, 1999b.

Brosch M, Budinger E, and Scheich H. Stimulus-related gamma oscillations in primate auditory cortex. *J Neurophysiol* 87: 2715–2725, 2002.

Brunel N and Wang XJ. What determines the frequency of fast network oscillations with irregular neural discharges? I. Synaptic dynamics and excitation-inhibition balance. *J Neurophysiol* 90: 415–430, 2003.

Buzsáki G. Hippocampal sharp waves: their origin and significance. *Brain Res* 398: 242–252, 1986.

Buzsáki G, Horváth Z, Urioste R, Hetke J, and Wise K. High-frequency network oscillation in the hippocampus. *Science* 256: 1025–1027, 1992.

Buzsáki G, Leung LW, and Vanderwolf CH. Cellular bases of hippocampal EEG in the behaving rat. *Brain Res* 287: 139–171, 1983.

Buzsáki G, Llinas RR, and Singer W. *Temporal Coding in the Brain.* Berlin: Springer-Verlag, 1994.

Castelo-Branco M, Neuenschwander S, and Singer W. Synchronization of visual responses between the cortex, lateral geniculate nucleus, and retina in the anesthetized cat. *J Neurosci* 18: 6395–6410, 1998.

Chrobak JJ and Buzsáki G. Operational dynamics in the hippocampal-entorhinal axis. *Neurosci Biobehav Rev* 22: 303–310, 1998.

Chrobak JJ, Lorincz A, and Buzsáki G. Physiological patterns in the hippocampo-entorhinal cortex system. *Hippocampus* 10: 457–465, 2000.

Cobb WA and Dawson GD. The latency and form in man of the occipital potentials evoked by bright flashes. *J Physiol* 152: 108–121, 1960.

Collins DR, Lang EJ, and Pare D. Spontaneous activity of the perirhinal cortex in behaving cats. *Neuroscience* 89: 1025–1039, 1999.

Cracco RQ and Cracco JB. Somatosensory evoked potential in man: far field potentials. *Electroencephalogr Clin Neurophysiol* 41: 460–466, 1976.

Cracco RQ and Cracco JB. Visual evoked potential in man: early oscillatory potentials. *Electroencephalogr Clin Neurophysiol* 45: 731–739, 1978.

Creutzfeldt O and Houchin J. Neuronal basis of EEG waves. In: *Handbook of Electroencephalography and Clinical Electrophysiology*, edited by Redmond A. Amsterdam: Elsevier, 1974.

Crone NE, Boatman D, Gordon B, and Hao L. Induced electrocorticographic gamma activity during auditory perception. *Clin Neurophysiol* 112: 565–582, 2001a.

Crone NE, Miglioretti DL, Gordon B, and Lesser RP. Functional mapping of human sensorimotor cortex with electrocorticographic spectral analysis. II. Event-related synchronization in the gamma band. *Brain* 121: 2301–2315, 1998.

Csépe V, Karmos G, and Molnár M. Evoked potential correlates of stimulus deviance during wakefulness and sleep in cat–animal model of mismatch negativity. *Electroencephalogr Clin Neurophysiol* 66: 571–578, 1987.

Csicsvari J, Jamieson B, Wise KD, and Buzsaki G. Mechanisms of gamma oscillations in the hippocampus of the behaving rat. *Neuron* 37: 311–322, 2003.

Curio G, Mackert BM, Burghoff M, Koetitz R, Abraham-Fuchs K, and Harer W. Localization of evoked neuromagnetic 600 Hz activity in the cerebral somatosensory system. *Electroencephalogr Clin Neurophysiol* 91: 483–487, 1994.

Davis PA. Effects of acoustic stimuli on the waking human brain. *J Neurophysiol* 2: 494–499, 1939.

Delorme A and Makeig S. EEGLAB: an open source toolbox for analysis of single-trial EEG dynamics including independent component analysis. *J Neurosci Methods* 134: 9–21, 2004.

Deouell LY, Bentin S, and Giard MH. Mismatch negativity in dichotic listening: evidence for interhemispheric differences and multiple generators. *Psychophysiology* 35: 355–365, 1998.

Deouell LY, Karns CM, Harrison TB, and Knight RT. Spatial asymmetries of auditory event-synthesis in humans. *Neurosci Lett* 335: 171–174, 2003.

Doeller CF, Optiz B, Mecklinger A, Krick RC, and Schroger E. Prefrontal cortex involvement in preattentive auditory deviance detection: neuroimaging and electrophysiological evidence. *Neuroimage* 87: 174–180, 2003.

Draguhn A, Traub RD, Schmitz D, and Jeffrey JG. Electrical coupling underlies high-frequency oscillations in the hippocampus in vitro. *Nature* 394: 189–192, 1998.

Durup G and Fessard A. L'électoencéphalogramme de l'homme. Observations psycho-physiologiques relatives à l'action des stimuli visuels et auditifs. *Ann Psychol* 36: 1–35, 1935.

Eguchi K and Satoh T. Relationship between positive sharp wave bursts and unitary discharges in the cat hippocampus during slow wave sleep. *Physiol Behav* 40: 497–499, 1987.

Elul R. The genesis of the EEG. *Int Rev Neurobiol* 15: 227–272, 1971.

Engel AK, Konig P, Kreiter AK, Schillen TB, and Singer W. Temporal coding in the visual cortex: new vistas on integration in the nervous system. *Trends Neurosci* 15: 218–226, 1992.

Fisher RS, Webber WR, Lesser RP, Arroyo S, and Uematsu S. High-frequency EEG activity at the start of seizures. *J Clin Neurophysiol* 9: 441–448, 1992.

Galambos R, Makeig S, and Talmachoff PJ. A 40-Hz auditory potential recorded from the human scalp. *Proc Natl Acad Sci USA* 78: 2643–2647, 1981.

Giard MH, Perrin F, Pernier J, and Bouchet P. Brain generators implicated in the processing of auditory stimulus deviance: a topographic event-related potential study. *Psychophysiology* 27: 627–640, 1990.

Godey B, Schwartz D, de Graaf JB, Chauvel P, and Liegeois-Chauvel C. Neuromagnetic source localization of auditory evoked fields and intracerebral evoked potentials: a comparison of data in the same patients. *Clin Neurophysiol* 112: 1850–1859, 2001.

Grenier F, Timofeev I, and Steriade M. Focal synchronization of ripples (80–200 Hz) in neocortex and their neuronal correlates. *J Neurophysiol* 86: 1884–1898, 2001.

Grenier F, Timofeev I, and Steriade M. Neocortical very fast oscillations (ripples, 80–200 Hz) during seizures: intracellular correlates. *J Neurophysiol* 89: 841–852, 2003.

Halgren E, Baudena P, Clarke JM, Heit G, Marinkovic K, Devaux B, Vignal JP, and Biraben A. Intracerebral potentials to rare target and distractor auditory and visual stimuli. I. Superior temporal plane and parietal lobe. *Electroencephalogr Clin Neurophysiol* 94: 191–220, 1995.

Hari R, Hamalainen M, Ilmoniemi R, Kaukoranta E, Reinikainen K, Sailminen J, Alho K, Näätänen R, and Sams M. Responses of the primary auditory cortex to pitch changes in a sequence of tone pips: neuromagnetic recordings in man. *Neurosci Lett* 50: 127–132, 1984.

Herculano-Houzel S, Munk MH, Neuenschwander S, and Singer W. Precisely synchronized oscillatory firing patterns require electroencephalographic activation. *J Neurosci* 19: 3992–4010, 1999.

Jääskeläinen IP, Ahveninen J, Bonmassar G, Dale AM, Ilmoniemi RJ, Levänen S, Lin FH, May P, Melcher J, Stufflebeam S, Tiitinen H, and Belliveau JW. Human posterior auditory cortex gates novel sounds to consciousness. *Proc Natl Acad Sci USA* 101: 6809–6814, 2004.

Javitt DC, Steinschneider M, Schroeder CE, Vaughan HG Jr, and Arezzo JC. Detection of stimulus deviance within primate primary auditory cortex: intracortical mechanisms of mismatch negativity (MMN) generation. *Brain Res* 667: 192–200, 1994.

Jones MS and Barth DS. Spatiotemporal organization of fast (>200 Hz) electrical oscillations in rat vibrissa/barrel cortex. *J Neurophysiol* 82: 1599–1609, 1999.

Jones MS and Barth DS. Effects of bicuculline methiodide on fast (>200 Hz) electrical oscillations in rat somatosensory cortex. *J Neurophysiol* 88: 1016–1025, 2002.

Kaiser J, Lutzenberger W, Ackerman H, and Birbaumer N. Dynamics of gamma-band activity induced by auditory pattern changes in humans. *Cereb Cortex* 12: 212–221, 2002.

Kanamori N. A spindle-like wave in the cat hippocampus: a novel vigilance level-dependent electrical activity. *Brain Res* 334: 180–182, 1985.

Kanamori N. Hippocampal minispindle wave in the cat: the different distribution of two types of waves. *Neurosci Res* 4: 152–156, 1986.

Knight RT, Hillyard SA, Woods D, and Neville HJ. The effects of frontal and temporal-parietal lesions on the auditory evoked potential in man. *Electroencephalogr Clin Neurophysiol* 2: 112–124, 1980.

Knight RT, Scabini D, Woods DL, and Clayworth C. The effects of lesions of superior temporal gyrus and inferior parietal lobe on temporal vertex components of the human AEP. *Electroencephalogr Clin Neurophysiol* 70: 499–509, 1988.

Kraus N, McGee T, Littman T, Nicol T, and King C. Nonprimary auditory thalamic representation of acoustic change. *J Neurophysiol* 72: 1270–1277, 1994.

Krause CM, Lang HA, Laine M, Helle SI, Kuusisto MJ, and Porn B. Event-related desynchronization evoked by auditory stimuli. *Brain Topogr* 7: 107–112, 1994.

Kropotov JD, Näätänen R, Sevostianov AV, Alho K, Reinikainen K, and Kropotova OV. Mismatch negativity to auditory stimulus change recorded directly from the human temporal cortex. *Psychophysiology* 32: 418–422, 1995.

Lachaux JP, George N, Tallon-Baudry C, Martinerie J, Hugueville L, Minotti L, Kahane P, and Renault B. The many faces of gamma band response to complex visual stimuli. *Neuroimage* 25: 491–501, 2005.

LeBeau FE, Traub RD, Monyer H, Whittington MA, and Buhl EH. The role of electrical signaling via gap junctions in the generation of fast network oscillations. *Brain Res Bull* 62: 3–13, 2003.

Lehtela L, Salmelin R, and Hari R. Evidence for reactive magnetic 10-Hz rhythm in the human auditory cortex. *Neurosci Lett* 222: 111–114, 1997.

Liasis A, Towell A, Alho K, and Boyd S. Intracranial identification of an electric frontal-cortex response to auditory stimulus change: a case study. *Brain Res Cogn Brain Res* 11: 227–233, 2001.

Liasis A, Towell A, and Boyd S. Intracranial evidence for differential encoding of frequency and duration discrimination responses. *Ear Hear* 21: 252–256, 2000.

Maciunas RJ, Berger MS, Copeland B, Mayberg MR, Selker R, and Allen GS. A technique for interactive image-guided neurosurgical intervention in primary brain tumors. *Neurosurg Clin N Am* 7: 245–266, 1996.

Maier N, Nimmrich V, and Draguhn A. Cellular and network mechanisms underlying spontaneous sharp wave-ripple complexes in mouse hippocampal slices. *J Physiol* 550: 873–887, 2003.

Makeig S. Auditory event-related dynamics of the EEG spectrum and effects of exposure to tones. *Electroencephalogr Clin Neurophysiol* 86: 283–293, 1993.

Makeig S, Westerfield M, Jung TP, Enghoff S, Townsend J, Courchesne E, and Sejnowski TJ. Dynamic brain sources of visual evoked responses. *Science* 295: 690–694, 2002.

Mingrino S, Coxe WS, Katz R, and Goldring S. The direct cortical response; associated events in pyramidal and muscle during development of movement and after-discharge. In: *Brain Mechanisms,* edited by Moruzzi G and Fessard Jasper H. Amsterdam: Elsevier, 1963.

Mitzdorf U. Current source-density method and application in cat cerebral cortex: investigation of evoked potentials and EEG phenomena. *Physiol Rev* 65: 37–100, 1985.

Munk MH and Neuenschwander S. High-frequency oscillations (20 to 120 Hz) and their role in visual processing. *J Clin Neurophysiol* 17: 341–360, 2000.

Näätänen R. *Attention and Brain Function.* Hillsdale, NJ: Lawrence Erlbaum, 1992.

Näätänen R and Picton T. The N1 wave of the human electric and magnetic response to sound: a review and an analysis of the component structure. *Psychophysiology* 24: 375–425, 1987.

Neuenschwander S, Castelo-Branco M, Baron J, and Singer W. Feedforward synchronization: propagation of temporal patterns along the retinothalamocortical pathway. *Philos Trans R Soc Lond B Biol Sci* 357: 1869–1876, 2002.

Neuenschwander S and Singer W. Long-range synchronization of oscillatory light responses in the cat retina and lateral geniculate nucleus. *Nature* 379: 728–732, 1996.

Nichols T and Hayasaka S. Controlling the familywise error rate in functional neuroimaging: a comparative review. *Stat Methods Med Res* 12: 419–446, 2003.

O'Keefe J. Place units in the hippocampus of the freely moving rat. *Exp Neurol* 51: 78–109, 1976.

O'Keefe J and Nadel L. *The Hippocampus as a Cognitive Map.* Oxford, UK: Clarendon Press, 1978.

Opitz R, Mecklinger A, von Cramon DY, and Kruggel F. Combining electrophysiological and hemodynamic measures of the auditory oddball. *Psychophysiology* 36: 142–147, 1999.

Opitz R, Rinne T, Mecklinger A, von Cramon DY, and Schroger E. Differential contribution of frontal and temporal cortices to auditory change detection: fMRI and ERP results. *Neuroimage* 15: 167–174, 2002.

Patton HD and Amassian VE. Single and multiple-unit analysis of cortical stage of pyramidal tract activation. *J Neurophysiol* 17: 345–363, 1954.

Pfurtscheller G and Aranibar A. Event-related cortical desynchronization detected by power measurements of scalp EEG. *Electroencephalogr Clin Neurophysiol* 42: 817–826, 1977.

Pfurtscheller G and Lopes da Silva FH. Event-related EEG/MEG synchronization and desynchronization: basic principles. *Clin Neurophysiol* 110: 1842–1857, 1999.

Picton TW, Hillyard SA, Krausz HI, and Galambos R. Human auditory evoked potentials. I. Evaluation of components. *Electroencephalogr Clin Neurophysiol* 36: 179–190, 1974.

Pincze Z, Lakatos P, Rajkai C, Ulbert I, and Karmos G. Separation of mismatch negativity and the N1 wave in the auditory cortex of the cat: a topographic study. *Clin Neurophysiol* 112: 778–784, 2001.

Rinne T, Alho K, Ilmoniemi RJ, Virtanen J, and Näätänen R. Separate time behaviors of the temporal and frontal mismatch negativity sources. *Neuroimage* 12: 14–19, 2000.

Rosburg T, Trautner P, Dietl T, Korzyukov OA, Boutros NN, Schaller C, Elger CE, and Kurthen M. Subdural recordings of the mismatch negativity (MMN) in patients with focal epilepsy. *Brain* 128: 819–828, 2005.

Sannita WG. Stimulus-specific oscillatory responses of the brain: a time/frequency-related coding process. *Clin Neurophysiol* 111: 565–583, 2000.

Scherg M, Vajsar J, and Picton TW. A source analysis of the late human auditory evoked potentials. *J Cogn Neurosci* 1: 336–355, 1989.

Serra JM, Giard MH, Yago E, Alho K, and Escera C. Bilateral contribution from frontal lobes to MMN. *Int J Psychophysiol* 30: 236–237, 1998.

Singer W. Synchronization of cortical activity and its putative role in information processing and learning. *Annu Rev Physiol* 55: 349–374, 1993.

Staba RJ, Brett-Green B, Paulsen M, and Barth DS. Effects of ventrobasal lesion and cortical cooling on fast oscillations (>200 Hz) in rat somatosensory cortex. *J Neurophysiol* 89: 2380–2388, 2003.

Staba RJ, Wilson CL, Bragin A, Fried I, and Engel J Jr. Quantitative analysis of high-frequency oscillations (80–500 Hz) recorded in human epileptic hippocampus and entorhinal cortex. *J Neurophysiol* 88: 1743–1752, 2002.

Sukov W and Barth DS. Three-dimensional analysis of spontaneous and thalamically evoked gamma oscillations in auditory cortex. *J Neurophysiol* 79: 2875–2884, 1998.

Sukov W and Barth DS. Cellular mechanisms of thalamically evoked gamma oscillations in auditory cortex. *J Neurophysiol* 85: 1235–1245, 2001.

Suzuki SS and Smith GK. Spontaneous EEG spikes in the normal hippocampus. II. Relations to synchronous burst discharges. *Electroencephalogr Clin Neurophysiol* 69: 532–534, 1988.

Suzuki T, Kobayashi K, and Hirabayashi M. Frequency composition of auditory middle responses. *Br J Audiol* 17: 1–4, 1983.

Tiihonen J, Hari R, Kajola M, Nousiainen U, and Vapalahti M. Magnetoencephalographic 10-Hz rhythm from the human auditory cortex. *Neurosci Lett* 129: 303–305, 1991.

Traub RD and Bibbig A. A model of high-frequency ripples in the hippocampus based on synaptic coupling plus axon-axon gap junctions between pyramidal neurons. *J Neurosci* 20: 2086–2093, 2000.

Traub RD, Cunningham MO, Gloveli T, LeBeau FE, Bibbig A, Buhl EH, and Whittington MA. GABA-enhanced collective behavior in neuronal axons underlies persistent gamma-frequency oscillations. *Proc Natl Acad Sci USA* 100: 11047–11052, 2003.

Traub RD, Schmitz D, Jefferys JG, and Draguhn A. High-frequency population oscillations are predicted to occur in hippocampal pyramidal neuronal networks interconnected by axoaxonal gap junctions. *Neuroscience* 92: 407–426, 1999.

Traub RD, Whittington MA, Buhl EH, LeBeau FE, Bibbig A, Boyd S, Cross H, and Baldeweg T. A possible role for gap junctions in generation of very fast EEG oscillations preceding the onset of, and perhaps initiating, seizures. *Epilepsia* 42: 153–170, 2001.

Vaughan HG Jr and Hull RC. Functional relation between stimulus intensity and photically evoked cerebral responses in man. *Nature* 206: 720–722, 1965.

Whittaker SG and Siegfried JB. Origin of wavelets in the visual evoked potential. *Electroencephalogr Clin Neurophysiol* 55: 91–101, 1983.

Wolpaw JR and Penry JK. A temporal component of the auditory evoked response. *Electroencephalogr Clin Neurophysiol* 39: 609–620, 1975.

Ylinen A, Bragin A, Nadasdy Z, Jando G, Szabo I, Sik A, and Buzsaki G. Sharp wave-associated high-frequency oscillation (200 Hz) in the intact hippocampus: network and intracellular mechanisms. *J Neurosci* 15: 30–46, 1995.

Zerlin S and Davis H. The variability of single evoked vertex potentials in man. *Electroencephalogr Clin Neurophysiol* 23: 468–472, 1967.